JOURNAL OF AGRICULTURAL AND FOOD CHEMISTRY

Akt/FOXO3a/SIRT1-Mediated Cardioprotection by *n*-Tyrosol against Ischemic Stress in Rat in Vivo Model of Myocardial Infarction: Switching Gears toward Survival and Longevity

SAMSON MATHEWS SAMUEL, MAHESH THIRUNAVUKKARASU, SURESH VARMA PENUMATHSA, DEBAYON PAUL, AND NILANJANA MAULIK*

Molecular Cardiology and Angiogenesis Laboratory, Department of Surgery, University of Connecticut Health Center, Farmington, Connecticut 06030

Moderate consumption of wine has been associated with decreased risk of cardiovascular events. Recently we have shown that white wine is equally as cardioprotective as red wine. However, unlike resveratrol (polyphenol in red wine), the white wine component, *n*-tyrosol [2-(4-hydroxyphenyl)ethanol] has not been explored for its cardioprotective effect and mechanism of action. Therefore, the present study was designed to evaluate the effect of tyrosol treatment (5 mg/kg/day for 30 days) on myocardial ischemic stress in a rat in vivo model of Myocardial Infarction (MI) and to identify key molecular targets involved in this mechanism. MI was induced by Left Anterior Descending (LAD) coronary artery ligation. Reduced infarct size (32.42 vs 48.03%) and cardiomyocyte apoptosis (171 vs 256 counts/100 HPF) were observed along with improvement in the myocardial functional parameters such as LVIDs (5.89 vs 6.58 mm), ejection fraction (51.91 vs 45.09%), and fractional shortening (28.46 vs 23.52%) as assessed by echocardiography in the tyrosol-treated animals when compared to the nontreated controls. We have also observed significant increase in the phosphorylation of Akt (1.4-fold), eNOS (3-fold) and FOXO3a (2.6-fold). In addition, tyrosol induced the expression of longevity protein SIRT1 (3.2-fold) in the MI group as compared to the non-treated MI control. Therefore tyrosol's SIRT1, Akt and eNOS activating power adds another dimension to the white wine research, because it adds a great link to the French paradox. In conclusion these findings suggest that tyrosol induces myocardial protection against ischemia related stress by inducing survival and longevity proteins that may be considered as anti-aging therapy for the heart. However, human intervention studies would be necessary before establishing any recommendations about dietary habits for tyrosol intake or administration of dietary supplements containing tyrosol.

KEYWORDS: Tyrosol; Akt; FOXO3a; SIRT1; eNOS; myocardial infarction; French paradox

INTRODUCTION

Over the past few years there have been significant advances in the therapy of ischemic heart diseases (IHD). However, there is still a major unmet need for better drugs/therapies for many IHD. Basic scientific research is being directed toward isolating and studying the mechanism of action of the active principles from naturally occurring compounds that are known to be cardioprotective. Mounting scientific evidence suggests that regular but moderate consumption of wine is associated with decreased risk of cardiovascular events (*1*). The cardioprotective effect of this natural ataractic agent has been related to the high content of biophenols (*2*). Recently we have reported that a red wine polyphenol, resveratrol, confers protection against myocardial injury caused by ischemia-reperfusion (IR), hypercholesterolemia, and diabetes (*3*−*5*). Bromelain (a proteolytic enzyme obtained from the stem of pineapple) mediated cardioprotection against IR injury through the phosphorylation of FOXO3a has been demonstrated (*6*). Moreover, we have recently reported for the first time that white wine pretreatment renders cardioprotection against myocardial IR injury via the Akt/FOXO pathway (*7*).

The FOXO proteins are known to be crucial regulators of a variety of cellular processes such as apoptosis, cell cycle progression, and oxidative stress resistance (*8*). The mammalian system has four FOXO family members, namely, FOXO1, FOXO3a, FOXO4, and FOXO6, which are known to be regulated by the Akt/PKB signaling pathway (*9, 10*). The FOXO transcription factors are known to induce the expression of pro-apoptotic proteins such as Bim and Fas-L while down-regulating

* Address correspondence to this author at the Molecular Cardiology and Angiogenesis Laboratory, Department of Surgery, UCONN Health Center, 263 Farmington Ave., Farmington, CT 06030 [telephone (860)-679-2857; fax (860)-679-2825; e-mail nmaulik@neuron.uchc.edu.

10.1021/jf802050h CCC: $40.75
Published on Web 10/01/2008

the expression of pro-survival proteins such as Bcl-X_L (*11*). Among the FOXO proteins, FOXO3a has been studied for its ability to mediate stress response by acting as an important sensor for cellular stresses (*11*−*13*). The transcriptional activity of FOXO3a is modulated not only by Akt but also by SIRT1 (*14, 15*). The mammalian sirtuin proteins (SIRT1−SIRT7) share a common catalytic domain with Sir2 (silent information regulator 2), an NAD^+-dependent deacetylase (*16*) that controls longevity in lower eukaryotes (an increase in Sir2 tends to increase the life expectancy of the cells) (*17*), of which the nuclear SIRT1 has the highest sequence similarity with Sir2 (*18*).

White wine is known to be rich in active components including shikimic acid, caffeic acid, *n*-tyrosol, and hydroxytyrosol (*7*). *n*-Tyrosol [2-(4-hydroxyphenyl)ethanol], a major component of olive oil, is a monophenolic active compound that has been shown to protect Caco-2 cells against oxidized LDL induced oxidative cellular damage, and exposure of these cells to *n*-tyrosol has been shown to prevent cell retraction caused by oxidized LDL (*19*). Vivancos et al. recently reported that *n*-tyrosol treatment reduced oxidized LDL stimulated oxidative stress in RAW 264.7 macrophages (*20*). Plotnikov et al. have shown that intragastric *n*-tyrosol treatment in male Wistar rats exhibited pronounced reduction in platelet aggregation and blood viscosity in these rats (*21*). It was also shown that intravenous administration of *n*-tyrosol 10 min prior to coronary occlusion in an in vivo acute myocardial ischemia model of Wistar rats significantly reduced the arrhythmic activity that occurs during myocardial ischemia and reperfusion (*22*). Hydroxytyrosol treatment of HepG2 cells improved the antioxidant defense system of these cells while increasing cellular integrity and stress resistance capabilities (*23*). Hydroxytyrosol has also been shown to protect the aorta against oxidative stress mediated impairment of nitric oxide (NO) and vessel relaxation (*24*). Moreover, increased myocardial apoptosis and infarct size have been reported in eNOS knockout mice, demonstrating the role of eNOS in cardioprotection (*25*). A review of the recent literature has demonstrated the protective effects of tyrosol; however, very few data exist on the molecular mechanisms involved in the protective effects of tyrosol. Therefore, in the present study we aimed at investigating whether and how *n*-tyrosol pretreatment could confer cardioprotection against an ischemic insult caused by permanent Left Anterior Descending (LAD) ligation in an in vivo model of rat Myocardial Infarction (MI).

MATERIALS AND METHODS

Animal Maintenance and Treatment. All animals used in this study received humane care in compliance with the principles of laboratory animal care formulated by the National Society for Medical Research and with the *Guide for the Care and Use of Laboratory Animals* prepared by the National Academy of Sciences and published by the National Institutes of Health (Publication 85-23, Revised 1996). The experimental protocol was approved by the Institutional Animal Care Committee of the University of Connecticut Health Center (Farmington, CT).

Experimental Design. Male Sprague−Dawley rats weighing 275−300 g were used for the study. The rats were randomized into four groups ($n = 24$ in each group): (1) control sham (CS); (2) tyrosol sham (TS); (3) control MI (CMI); and (4) tyrosol MI (TMI). The experimental rats were gavaged with *n*-tyrosol [2-(4-hydroxyphenyl)ethanol] (Sigma-Aldrich, St. Loius, MO) at a dosage of 5 mg/kg/rat/day for 30 days. MI was induced by permanent LAD coronary artery ligation. The myocardial infarct size was measured 24 h after MI, whereas the protein expression profile for the phosphorylated proteins (p-Akt, p-eNOS, and p-FOXO3a) and the longevity protein SIRT1 was observed in the left ventricular tissue 8 h and 4 days after MI, respectively. The cardiac functions and the extent of cardiac fibrosis were measured at 45 days after the MI.

Surgical Procedure. The experimental model has been described previously (*3, 26*). Briefly, under anesthesia with ketamine (100 mg/kg, ip) and xylazine (10 mg/kg, ip) and artificial ventilation, the heart was exposed via left lateral thoracotomy followed by pericardiectomy. The LAD was ligated permanently with 6-0 polypropylene suture. Sham-operated rats underwent thoracotomy and pericardiectomy followed by passing the suture under the LAD without ligation. After positive end-diastolic pressure was applied to fully inflate the lung, the chest was closed with 4-0 polypropylene suture. Cefazolin (25 mg/kg, ip) was administered as a preoperative antibiotic cover. After surgery, analgesic buprenorphine (0.1 mg/kg, sc) was given, and the animals were weaned from the respirator and then placed on a heating pad for recovery.

Assessment of Infarct Size. Twenty-four hours after MI, infarct size was measured in eight horizontal sections between the point of ligation and the apex. The area at risk (AAR) was recognized as the area not perfused with 50% Unisperse Blue (Ciba-Geigy, Glen Ellyn, IL), whereas the noninfarcted and infarcted areas were demarcated after incubation with 1% triphenyltetrazolium chloride (Sigma-Aldrich). With the use of Scion image software (Scion Corp.), the volumes of both infarcted myocardium and the AAR were calculated. Infarct size was reported as a percentage of the AAR (*3, 26*).

Cardiomyocyte Apoptosis. The formaldehyde-fixed left ventricle was embedded in paraffin, cut into transverse sections (4 μm thick), and deparaffinized with a graded series of histoclear and ethanol solutions. Immunohistochemical detection of apoptotic cells was carried out using TUNEL reaction using an In Situ Cell Death Detection Kit and fluorescein as per the kit protocol (Roche Diagnostics, Mannheim, Germany). In brief, the TUNEL reaction preferentially labels DNA strand breaks generated during apoptosis, which can be identified by labeling free 3′-OH termini with modified nucleotides in an enzymatic reaction catalyzed by terminal deoxynucleotidyltransferase (TdT). Fluorescein labels incorporated in nucleotide polymers are detected by fluorescence microscopy. The sections were washed three times in PBS, blocked with 10% normal goat serum in 1% BSA in PBS, and incubated with mouse monoclonal anti-α-sarcomeric actin (Sigma, St. Louis, MO) followed by staining with TRITC-conjugated rabbit anti-mouse IgG (1:200 dilution, Sigma). After incubation, the sections were rinsed three times in PBS and mounted with Vectashield mounting medium (Vector, Burlingame, CA). The sections were observed, and images were captured using a confocal laser Zeiss LSM 410 microscope. For quantitative purposes, the number of TUNEL-positive cardiomyocytes was counted on 100 high-power fields (HPF) (*6*).

Isolation of Nuclear and Cytosolic Protein Fractions. The myocardial tissue for analysis was harvested from the risk zone or border zone of the left ventricle adjacent to the infarct (avoiding any infarcted tissue). The protein was isolated according to the kit protocol of the CelLytic NuCLEAR Extraction Kit from Sigma. In brief, 100 mg of tissue was homogenized in 1 mL of buffer containing 100 mM HEPES (pH 7.9) with 15 mM $MgCl_2$, 100 mM KCl, and 0.1 M DTT solution and centrifuged at 10000*g* for 20 min. The supernatant containing the cytosolic fraction was transferred to a fresh tube. The pellet was resuspended in 150 μL of extraction buffer containing 1.5 μL of 0.1 M DTT and 1.5 μL of protease inhibitor cocktail (104 mM AEBSF, 80 μM aprotinin, 4 mM bestatin, 1.4 mM E-64, 2 mM leupeptin, and 1.5 mM pepstatin A). The solution was allowed to stand on ice for 30 min with shaking at brief intervals followed by centrifugation at 20000*g* for 5 min. The supernatant was transferred to a clean chilled tube and contained the nuclear protein fraction. The cytosolic and nuclear total protein concentrations were determined using a bicinchoninic acid protein assay kit (Pierce, Rockville, IL) (*6, 7*).

Western Blot Analysis for Phosphorylated Akt, FOXO3a, eNOS, and Nuclear SIRT1. To quantify the p-Akt, p-FOXO3a, p-eNOS (8 h sample/cytosolic fraction) and SIRT1 (4 day sample/nuclear fraction), the standard SDS-PAGE Western blot technique was performed (*3, 5*−*7, 27*). The proteins were run on polyacrylamide electrophoresis gels (SDS-PAGE) typically using 7% for p-eNOS and SIRT1 and 10% for p-Akt and p-FOXO3a. The antibodies for p-eNOS (the phosphorylation site

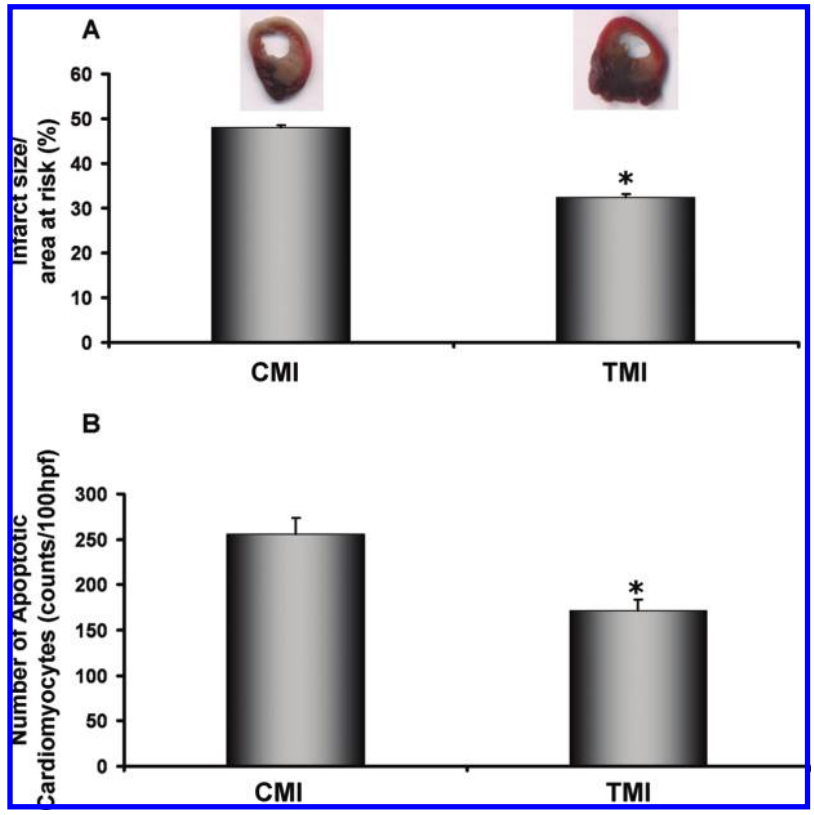

Figure 1. Effect of *n*-tyrosol on (**A**) infarct size [graphical representation of infarct size in percent area at risk between the control MI and *n*-tyrosol-treated MI groups 24 h after LAD ligation; values are mean ± SEM ($n = 6$)] and (**B**) cardiomyocyte apoptosis [graphical representation of cardiomyocyte apoptosis between the control MI and *n*-tyrosol-treated MI groups 24 h after LAD ligation]. *, $p < 0.05$, represents *n*-tyrosol-treated MI (TMI) compared with control MI (CMI) group.

is specific to serine-1177, 1:500), eNOS (1:500), p-Akt (the phosphorylation site is specific to serine-473, 1:500), Akt (1:500), p-FOXO3a (the phosphorylation site is specific to threonine-32, 1:500), and FOXO3a (1:500) were purchased from Cell Signaling Technology, Danvers, MA, and that for SIRT1 (1:250) was from Santa Cruz Biotechnology (Santa Cruz, CA). Primary antibody binding was visualized by HRP-conjugated secondary antibodies and enhanced chemiluminescence (ECL).

Assessment of Cardiac Fibrosis (Masson's Trichrome Staining). To determine the effect of *n*-tyrosol treatment on cardiac fibrosis, the collagenous fibrotic area of the heart was stained by Masson's trichrome staining protocol. The rats were sacrificed 45 days after the surgical procedure; hearts were removed and fixed overnight in 4% paraformaldehyde. After fixation, paraffin-embedded sections (4 μm thick) were made, and the extent of fibrosis was analyzed using Masson's trichrome staining (*28*). In brief, the paraffin sections were deparaffinized in histoclear and rehydrated using sequential passage through 100, 95, 80, and 70% ethanol for 6 min each followed by washing in distilled water three times. The slides were then stained with Weigert's iron hematoxylin for 10 min and placed under tap water for 10 min. The sections were again washed in distilled water and then stained with Biebrich scarlet-acid fuschin solution for 15 min, in phosphomolybdic−phosphotungstic acid solution for 15 min and aniline blue solution, and stained for 10 min. The sections were rinsed briefly in distilled water and were treated with 1% acetic acid solution for 5 min. After a final wash in distilled water, the sections were dehydrated through a sequential gradient of 70−100% alcohol followed by histoclear wash and then mounted using Permount. The heart tissue sections were digitally imaged in high-pixel resolution on an Epson Scanner, and enlarged images were captured using a phase contrast microscope with a high-resolution digital camera (Olympus).

Echocardiography. At 45 days after MI, rats were sedated using isoflurane (3%, inhaled). When adequately sedated, the rat was secured with tape in the supine position in a custom-built platform designed to maintain the rat's natural body shape after fixation. The hair on the chest wall was removed with a chemical hair remover. Ultrasound gel was spread over the precordial region, and ultrasound biomicroscopy (UBM) (Vevo 770, Visual-Sonics Inc., Toronto, ON, Canada) with a 25-MHz transducer was used to visualize the left ventricle. The left ventricle was analyzed in apical, parasternal long axis, and parasternal short axis views for left ventricular (LV) systolic function, LV cavity diameter, wall thickness, diastolic function, and LV end-systolic and end-diastolic volume determination. Two-dimensional directed M-mode images of the LV short axis were taken just below the level of the papillary muscles for analyzing ventricular wall thickness and chamber diameter. All left ventricular parameters were measured according to the modified American Society of Echocardiography recommended guidelines. Ejection fraction (EF) and fractional shortening (FS) were assessed for left ventricular systolic function. All measurements represent the mean of at least three consecutive cardiac cycles. Throughout the procedure ECG, respiratory rate, and heart rate were monitored as previously described (*6, 27, 29*).

Statistical Analysis. The values are expressed as means ± SEM. The ANOVA test was first carried out followed by Bonferroni correction to test for any differences between the mean values of all groups. The results were considered to be significant if $p < 0.05$.

RESULTS

Effect of *n*-Tyrosol on Infarct Size and Cardiomyocyte Apoptosis. Quantitative analysis indicated that tyrosol treatment significantly reduced myocardial infarct size 24 h after MI compared with the nontreated group. Tyrosol treatment reduced the infarct size approximately to 32% as compared to 48% in the CMI group (**Figure 1A**). A significant decrease in cardiomyocyte apoptosis was also observed in the TMI group as compared to the CMI group (171 vs 256 counts/100 HPF) (**Figure 1B**).

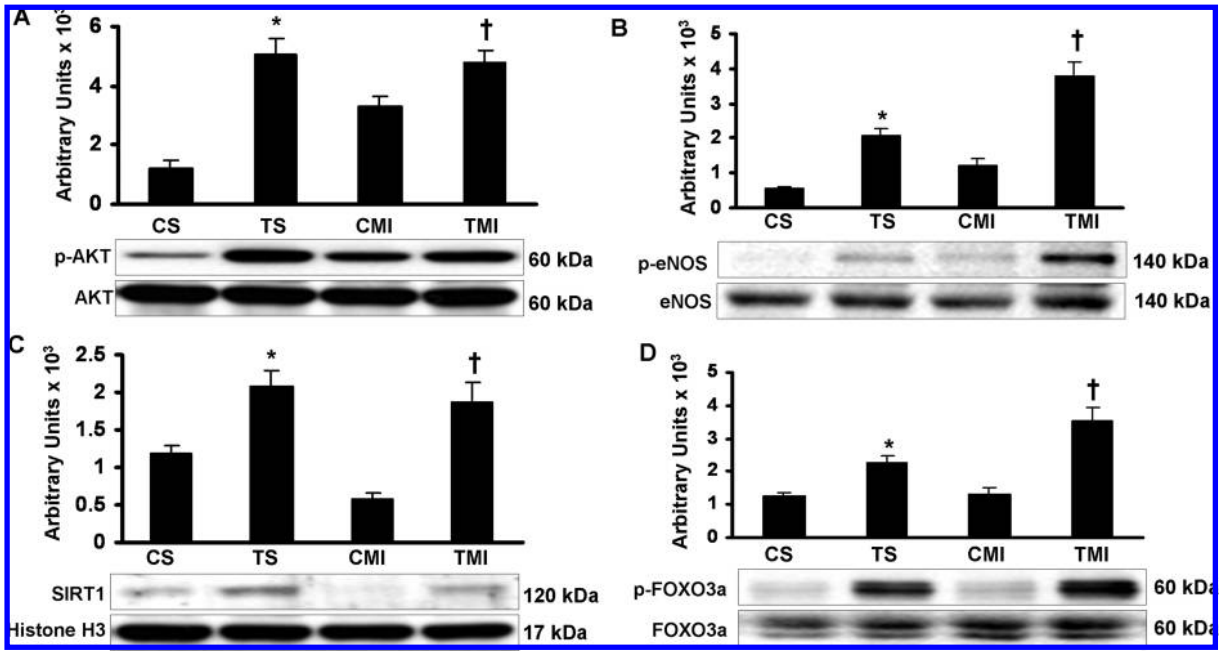

Figure 2. Representative Western blots showing the protein expression of p-Akt (**A**), p-eNOS (**B**), SIRT1 (**C**), and p-FOXO3a (**D**). Akt, eNOS, histone-H3, and FOXO3a were used as the respective loading controls. Graphs represent the quantitative comparison between the groups. ∗, $p < 0.05$, represents *n*-tyrosol-treated sham (TS) group compared with control sham (CS) group; †, $p < 0.05$, represents *n*-tyrosol-treated MI (TMI) group compared with control MI (CMI) group.

Effect of *n*-Tyrosol on Phosphorylation of Akt, eNOS, and FOXO3a. The phosphorylation status of Akt, eNOS, and FOXO3a proteins was observed after 8 h of LAD occlusion. *n*-Tyrosol treatment has shown significant increase in the p-Akt (**Figure 2A**) in both TS and TMI groups (4- and 1.4-fold) as compared to the corresponding CS and CMI groups. Similarly, *n*-tyrosol treatment has shown significant increase in the p-eNOS level (**Figure 2B**) in both TS and TMI groups (3.5- and 3-fold) as compared to corresponding CS and CMI groups. The p-FOXO3a levels (**Figure 2D**) in TS and TMI were also found to be significantly increased (1.8- and 2.6-fold) as compared to corresponding controls. No significant difference was observed in the nonphosphorylated protein levels of these proteins.

Effect of *n*-Tyrosol on SIRT1 Expression. The levels of nuclear longevity protein SIRT1 were examined in the groups 4 days after MI. There was a significant decrease in the SIRT1 expression in the CMI group as compared to the CS group. However, *n*-tyrosol treatment has shown a significant increase in the levels of nuclear SIRT1 (**Figure 2C**) in the TS (1.7-fold) and TMI (3.2-fold) as compared to the respective controls CS and CMI. Nuclear histone H3 was used as the loading control.

Effect of *n*-Tyrosol on Cardiac Fibrosis. The *n*-tyrosol-treated MI group demonstrated significantly reduced collagen staining and fibrosis compared with the respective nontreated control. **Figure 3D** shows a smaller infarct with less fibrosis in the *n*-tyrosol-treated TMI heart when compared with larger infarct with fibrosis and ventricular dilatation in a CMI heart (**Figure 3C**). Panels **E** and **F** of **Figure 3** show enlarged images of the infarct and peri-infarct regions of CMI and TMI groups, respectively. A significant increase in regions of viable cardiac muscle was observed in the infarct and peri-infarct regions of the *n*-tyrosol-treated MI group as compared with the nontreated control (**Figure 3E**,**F**). Panels **A** and **B** of **Figure 3** represent the nontreated and *n*-tyrosol-treated sham, respectively, with no significant fibrosis.

Effect of *n*-Tyrosol on Myocardial Functions by Echocardiography. There were no significant differences at baseline between treated and nontreated groups in the echocardiographic measurements either in cardiac structure or in function. Cardiac function measured at 45 days after MI showed increased left ventricular functions in the *n*-tyrosol-treated group as compared with that in control animals. Compared with the sham groups (CS and TS), decreased LV function and increased LV dilation were observed in both CMI and TMI groups after LAD ligation. The ejection fraction (51.91 vs 45.09%, **Figure 4C**) and fractional shortening (28.46 vs 23.52%, **Figure 4D**) of the left ventricle were significantly increased in the TMI group compared to the CMI group. As seen in **Figure 4A**, representative M-mode images demonstrated increased systolic and diastolic LV chamber dimensions after MI. The left ventricular chamber was dilated in the CMI compared to TMI as assessed by measuring LVIDs (6.58 vs 5.89 mm, **Figure 4B**). There was a compensatory increase in the posterior (LVPW) and lateral wall systolic thickness in the tyrosol-treated group as compared to the nontreated group (data not shown).

DISCUSSION

In the present study we have documented for the first time that white wine component *n*-tyrosol [2-(4-hydroxyphenyl)ethanol] renders cardioprotection against the ischemic stress induced by myocardial infarction in a rat in vivo LAD occlusion (MI) model. *n*-Tyrosol pretreatment significantly reduced the myocardial infarct size and the extent of cardiomyocyte apoptosis followed by decreased ventricular remodeling as evidenced by the significant reduction in the collagenous fibrotic tissue and improvement in the left ventricular myocardial functions in conjunction with a significant increase in the levels of phosphorylated forms of Akt, eNOS, and FOXO3a along with increased expression of nuclear SIRT1 in the *n*-tyrosol-administered groups as compared to untreated controls.

Serine 473 (Ser^{473}) phosphorylated active Akt is known to play a critical role in promoting cell survival by phosphorylation of its downstream target molecules such as the FOXO proteins, a subclass of the forkhead group of transcription factors (*8, 9*).

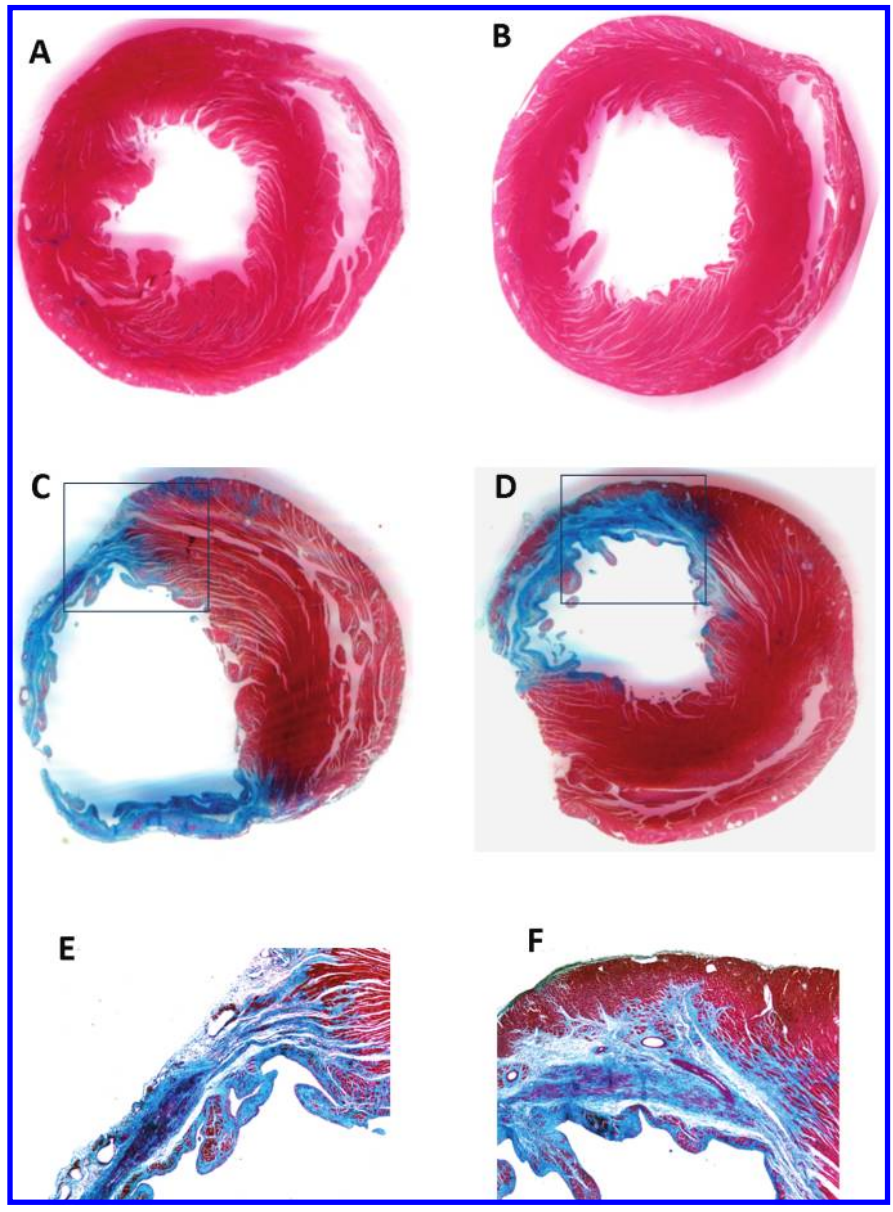

Figure 3. Representative images showing effect of *n*-tyrosol treatment on collagenous fibrotic area of the heart 45 days after surgical procedure (Masson's trichrome staining). Images **A** and **B** represent the control sham (CS) group and *n*-tyrosol-treated sham (TS) group, respectively, with no significant fibrosis, whereas images **C** and **D** represent the collagenous fibrotic staining in blue in the CMI and TMI groups, respectively. Images **E** and **F** show enlarged images of regions of the infarct and peri-infarct area of the control MI group (CMI) and *n*-tyrosol-treated MI (TMI) groups, respectively, showing viable cardiac tissue in the TMI group (the area that has been focused and zoomed in on to obtain images **E** and **F** are boxed on images **C** and **D**, respectively).

Akt activation not only increased cell survivability in the in vivo model but also improved regional and overall myocardial function (*30*). Phosphorylation of FOXO3a by Akt in the cytoplasm has been shown to sequester FOXO3a in the cytoplasm and enhance its degradation (*11*), whereas the same event of phosphorylation in the nucleus significantly reduces the DNA binding activity of FOXO3a and creates 14-3-3 protein docking sites on it, thereby facilitating its nuclear export and subsequent entry into the proteasomal degradation pathway in the cytosol (*31*). Thus, phosphorylation of FOXO3a by Akt has been shown to have an effect on the transcriptional regulation of FOXO3a-dependent genes, thereby inhibiting Bim- and Fas-L-dependent apoptosis. In the present study, the increase in the phosphorylation of Akt and FOXO3a thus corresponds to the reduced myocardial infarct size, less collagenous fibrotic tissue, and increased islands of viable cardiac muscle as a result of increased cell survivability in the *n*-tyrosol-treated MI group as compared to the nontreated control MI group.

SIRT1 has been shown to regulate stress response and survival of cells by modulating the FOXO3a transcription factors (*32*). The red wine polyphenol resveratrol was also shown to increase SIRT1 activity in favor of cell survival (*33*). SIRT1 is known to localize in the nucleus irrespective of the cellular stress status, whereas cytoplasmic FOXO3a relocates to the nucleus in response to various stress stimuli (*14*). SIRT1 has been shown to interact with phosphorylated FOXO3a and deacetylate it in the nucleus (*34*). This interaction increased FOXO3a's capability of inducing cell cycle arrest, resisting stress, and inducing DNA repair mechanisms while inhibiting FOXO3a's ability to induce apoptosis (*34*−*36*). Thus, the FOXO3a-dependent responses toward stress may be modulated away from cell death and toward stress resistance by the nuclear SIRT1. In the present

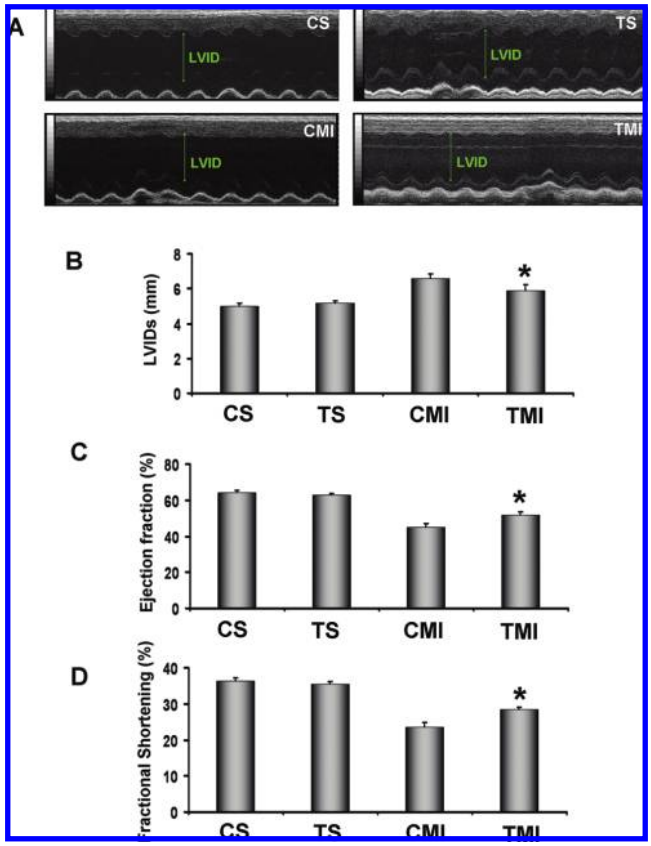

Figure 4. Effect of *n*-tyrosol on cardiac functions by echocardiography: (**A**) representative M-mode images of control sham (CS), *n*-tyrosol-treated sham (TS), control myocardial infarction (CMI), and *n*-tyrosol-treated myocardial infarction group (TMI) 45 days after the surgical procedure. Graph represents the left ventricular internal diameter in systole (LVIDs) in mm (**B**), % ejection fraction (EF) (**C**), and % fractional shortening (FS) (**D**) in CS, TS, CMI, and TMI 45 days after the surgical procedure. Values are mean ± SEM ($n = 6$). ∗, $p < 0.05$, represents TMI compared with CMI group.

study, we have documented the effect of *n*-tyrosol treatment on the levels of nuclear SIRT1. We have observed significant increase in the expression of nuclear SIRT1 in the tyrosol-treated groups as compared to the respective nontreated controls.

We have also observed a significant increase in the serine 1177 (Ser^{1177}) phosphorylation of eNOS in the tyrosol-treated group as compared to the nontreated controls. Reports have documented that active Akt phosphorylates and activates eNOS, thereby reducing the myocardial infarct size in a rat model of ischemia reperfusion injury (*37, 38*). It was shown that eNOS inhibition and reduction of NO levels compromised endothelial-dependent vasodilation and ventricular function in eNOS-deficient mice, whereas transgenic expression of eNOS has been shown to attenuate congestive heart failure and myocardial IR injury in mice (*39*−*41*). Moreover, FOXO3a has been known to be a transcriptional repressor of eNOS (*42*).

Therefore, the tyrosol-induced phosphorylation of Akt, subsequent phosphorylation of FOXO3a and eNOS, and increase in the expression of SIRT1 should have played a critical role in increasing cell survivability, bringing about significant reduction of myocardial infarct size due to reduced apoptosis (**Figure 1**), less collagenous fibrotic tissue (**Figure 3D**), increased regions of viable cardiac muscle (**Figure 3F**), and improvement in the left ventricular functional parameters (**Figure 4**) in the *n*-tyrosol-treated MI group as compared to the nontreated controls. The inhibition of FOXO3a by phosphorylation also might explain the increased levels of p-eNOS, because FOXO3a is considered to be a transcriptional repressor of eNOS.

In conclusion, we have demonstrated for the first time that a white wine component, tyrosol, induces myocardial protection against ischemia-induced stress by significantly reducing the myocardial infarct size and improving the left ventricular myocardial functions through the activation of Akt, eNOS, and SIRT1, which in turn may coordinate in shifting the FOXO3a-dependent stress response away from inducing a programmed cell death response but toward stress resistance and longevity. The present study is of significant clinical importance because it has elucidated a possible mechanism for the cardioprotective effect of tyrosol, prompting the development of a new drug to combat IHD while also revealing potential therapeutic molecular targets such as FOXO3a and SIRT1 that can be modulated to precondition the heart to overcome an ischemic stress.

LITERATURE CITED

(1) Di Castelnuovo, A.; Rotondo, S.; Iacoviello, L.; Donati, M. B.; De Gaetano, G. Meta-analysis of wine and beer consumption in relation to vascular risk. *Circulation* **2002**, *105* (24), 2836–2844.

(2) Williams, M. J.; Sutherland, W. H.; Whelan, A. P.; McCormick, M. P.; de Jong, S. A. Acute effect of drinking red and white wines on circulating levels of inflammation-sensitive molecules in men with coronary artery disease. *Metabolism* **2004**, *53* (3), 318–323.

(3) Penumathsa, S. V.; Thirunavukkarasu, M.; Koneru, S.; Juhasz, B.; Zhan, L.; Pant, R.; Menon, V. P.; Otani, H.; Maulik, N. Statin and resveratrol in combination induces cardioprotection against myocardial infarction in hypercholesterolemic rat. *J. Mol. Cell. Cardiol.* **2007**, *42* (3), 508–516.

(4) Ray, P. S.; Maulik, G.; Cordis, G. A.; Bertelli, A. A.; Bertelli, A.; Das, D. K. The red wine antioxidant resveratrol protects isolated rat hearts from ischemia reperfusion injury. *Free Radical Biol. Med.* **1999**, *27* (1−2), 160–169.

(5) Thirunavukkarasu, M.; Penumathsa, S. V.; Koneru, S.; Juhasz, B.; Zhan, L.; Otani, H.; Bagchi, D.; Das, D. K.; Maulik, N. Resveratrol alleviates cardiac dysfunction in streptozotocin-induced diabetes: role of nitric oxide, thioredoxin, and heme oxygenase. *Free Radical Biol. Med.* **2007**, *43* (5), 720–729.

(6) Juhasz, B.; Thirunavukkarasu, M.; Pant, R.; Zhan, L.; Penumathsa, S. V.; Secor, E. R., Jr.; Srivastava, S.; Raychaudhuri, U.; Menon, V. P.; Otani, H.; Thrall, R. S.; Maulik, N. Bromelain induces cardioprotection against ischemia-reperfusion injury through Akt/FOXO pathway in rat myocardium. *Am. J. Physiol. Heart Circ. Physiol.* **2008**, *294* (3), H1365–H1370.

(7) Thirunavukkarasu, M.; Penumathsa, S. V.; Samuel, S. M.; Akita, Y.; Zhan, L.; Bertelli, A. A. E.; Das, D. K.; Maulik, N. White wine mediated cardioprotection against ischemia-reperfusion injury is through activation of Akt/Foxo and eNOS pathway. *J. Agric. Food Chem.* **2008**, *56*, 6733–6739.

(8) Carter, M. E.; Brunet, A. FOXO transcription factors. *Curr. Biol.* **2007**, *17* (4), R113–R114.

(9) Brunet, A.; Bonni, A.; Zigmond, M. J.; Lin, M. Z.; Juo, P.; Hu, L. S.; Anderson, M. J.; Arden, K. C.; Blenis, J.; Greenberg, M. E. Akt promotes cell survival by phosphorylating and inhibiting a Forkhead transcription factor. *Cell* **1999**, *96* (6), 857–868.

(10) Jacobs, F. M.; van der Heide, L. P.; Wijchers, P. J.; Burbach, J. P.; Hoekman, M. F.; Smidt, M. P. FoxO6, a novel member of the FoxO class of transcription factors with distinct shuttling dynamics. *J. Biol. Chem.* **2003**, *278* (38), 35959–35967.

(11) Lam, E. W.; Francis, R. E.; Petkovic, M. FOXO transcription factors: key regulators of cell fate. *Biochem. Soc. Trans.* **2006**, *34* (Part 5), 722–726.

(12) Sunters, A.; Fernandez de Mattos, S.; Stahl, M.; Brosens, J. J.; Zoumpoulidou, G.; Saunders, C. A.; Coffer, P. J.; Medema, R. H.; Coombes, R. C.; Lam, E. W. FoxO3a transcriptional regulation of Bim controls apoptosis in paclitaxel-treated breast cancer cell lines. *J. Biol. Chem.* **2003**, *278* (50), 49795–49805.

(13) Sunters, A.; Madureira, P. A.; Pomeranz, K. M.; Aubert, M.; Brosens, J. J.; Cook, S. J.; Burgering, B. M.; Coombes, R. C.; Lam, E. W. Paclitaxel-induced nuclear translocation of FOXO3a in breast cancer cells is mediated by c-Jun NH_2-terminal kinase and Akt. *Cancer Res.* **2006**, *66* (1), 212–220.
(14) Giannakou, M. E.; Partridge, L. The interaction between FOXO and SIRT1: tipping the balance towards survival. *Trends Cell Biol.* **2004**, *14* (8), 408–412.
(15) Nemoto, S.; Fergusson, M. M.; Finkel, T. Nutrient availability regulates SIRT1 through a forkhead-dependent pathway. *Science* **2004**, *306* (5704), 2105–2108.
(16) Imai, S.; Armstrong, C. M.; Kaeberlein, M.; Guarente, L. Transcriptional silencing and longevity protein Sir2 is an NAD-dependent histone deacetylase. *Nature* **2000**, *403* (6771), 795–800.
(17) Tissenbaum, H. A.; Guarente, L. Increased dosage of a sir-2 gene extends lifespan in *Caenorhabditis elegans*. *Nature* **2001**, *410* (6825), 227–230.
(18) Frye, R. A. Phylogenetic classification of prokaryotic and eukaryotic Sir2-like proteins. *Biochem. Biophys. Res. Commun.* **2000**, *273* (2), 793–798.
(19) Giovannini, C.; Straface, E.; Modesti, D.; Coni, E.; Cantafora, A.; De Vincenzi, M.; Malorni, W.; Masella, R. Tyrosol, the major olive oil biophenol, protects against oxidized-LDL-induced injury in Caco-2 cells. *J. Nutr.* **1999**, *129* (7), 1269–77.
(20) Vivancos, M.; Moreno, J. J. Effect of resveratrol, tyrosol and beta-sitosterol on oxidised low-density lipoprotein-stimulated oxidative stress, arachidonic acid release and prostaglandin E2 synthesis by RAW 264.7 macrophages. *Br. J. Nutr.* **2008**, *99* (6), 1199–1207.
(21) Plotnikov, M. B.; Chernysheva, G. A.; Smol'yakova, V. I.; Maslov, M. Y.; Cherkashina, I. V.; Krysin, A. P.; Sorokina, I. V.; Tolstikova, T. G. Effect of *n*-tyrosol on blood viscosity and platelet aggregation. *Bull. Exp. Biol. Med.* **2007**, *143* (1), 61–3.
(22) Chernyshova, G. A.; Plotnikov, M. B.; Smol'yakova, V. I.; Golubeva, I. V.; Aliev, O. I.; Tolstikova, T. G.; Krysin, A. P.; Sorokina, I. V. Antiarrhythmic activity of *n*-tyrosol during acute myocardial ischemia and reperfusion. *Bull. Exp. Biol. Med.* **2007**, *143* (6), 689–691.
(23) Goya, L.; Mateos, R.; Bravo, L. Effect of the olive oil phenol hydroxytyrosol on human hepatoma HepG2 cells. Protection against oxidative stress induced by *tert*-butylhydroperoxide. *Eur. J. Nutr.* **2007**, *46* (2), 70–78.
(24) Rietjens, S. J.; Bast, A.; de Vente, J.; Haenen, G. R. The olive oil antioxidant hydroxytyrosol efficiently protects against the oxidative stress-induced impairment of the NObullet response of isolated rat aorta. *Am. J. Physiol. Heart Circ. Physiol.* **2007**, *292* (4), H1931–H1936.
(25) Jones, S. P.; Girod, W. G.; Palazzo, A. J.; Granger, D. N.; Grisham, M. B.; Jourd'Heuil, D.; Huang, P. L.; Lefer, D. J. Myocardial ischemia-reperfusion injury is exacerbated in absence of endothelial cell nitric oxide synthase. *Am. J. Physiol.* **1999**, *276* (5 Part 2), H1567–H1573.
(26) Kaga, S.; Zhan, L.; Matsumoto, M.; Maulik, N. Resveratrol enhances neovascularization in the infarcted rat myocardium through the induction of thioredoxin-1, heme oxygenase-1 and vascular endothelial growth factor. *J. Mol. Cell. Cardiol.* **2005**, *39* (5), 813–822.
(27) Penumathsa, S. V.; Koneru, S.; Thirunavukkarasu, M.; Zhan, L.; Prasad, K.; Maulik, N. Secoisolariciresinol diglucoside: relevance to angiogenesis and cardioprotection against ischemia-reperfusion injury. *J. Pharmacol. Exp. Ther.* **2007**, *320* (2), 951–959.
(28) Edelberg, J. M.; Lee, S. H.; Kaur, M.; Tang, L.; Feirt, N. M.; McCabe, S.; Bramwell, O.; Wong, S. C.; Hong, M. K. Platelet-derived growth factor-AB limits the extent of myocardial infarction in a rat model: feasibility of restoring impaired angiogenic capacity in the aging heart. *Circulation* **2002**, *105* (5), 608–613.
(29) Koneru, S.; Penumathsa, S. V.; Thirunavukkarasu, M.; Vidavalur, R.; Zhan, L.; Singal, P. K.; Engelman, R. M.; Das, D. K.; Maulik, N. Sildenafil mediated neovascularization and protection against myocardial ischemia reperfusion injury in rats: probable role of Vegf/angiopoietin-1. *J. Cell. Mol. Med.* **2008**, in press.
(30) Matsui, T.; Tao, J.; del Monte, F.; Lee, K. H.; Li, L.; Picard, M.; Force, T. L.; Franke, T. F.; Hajjar, R. J.; Rosenzweig, A. Akt activation preserves cardiac function and prevents injury after transient cardiac ischemia in vivo. *Circulation* **2001**, *104* (3), 330–335.
(31) Webster, K. A. Aktion in the nucleus. *Circ. Res.* **2004**, *94* (7), 856–859.
(32) Michishita, E.; Park, J. Y.; Burneskis, J. M.; Barrett, J. C.; Horikawa, I. Evolutionarily conserved and nonconserved cellular localizations and functions of human SIRT proteins. *Mol. Biol. Cell* **2005**, *16* (10), 4623–4635.
(33) Dillin, A.; Kelly, J. W. Medicine. The yin-yang of sirtuins. *Science* **2007**, *317* (5837), 461–462.
(34) Brunet, A.; Sweeney, L. B.; Sturgill, J. F.; Chua, K. F.; Greer, P. L.; Lin, Y.; Tran, H.; Ross, S. E.; Mostoslavsky, R.; Cohen, H. Y.; Hu, L. S.; Cheng, H. L.; Jedrychowski, M. P.; Gygi, S. P.; Sinclair, D. A.; Alt, F. W.; Greenberg, M. E. Stress-dependent regulation of FOXO transcription factors by the SIRT1 deacetylase. *Science* **2004**, *303* (5666), 2011–2015.
(35) Tran, H.; Brunet, A.; Grenier, J. M.; Datta, S. R.; Fornace, A. J., Jr.; DiStefano, P. S.; Chiang, L. W.; Greenberg, M. E. DNA repair pathway stimulated by the forkhead transcription factor FOXO3a through the Gadd45 protein. *Science* **2002**, *296* (5567), 530–534.
(36) Furukawa-Hibi, Y.; Yoshida-Araki, K.; Ohta, T.; Ikeda, K.; Motoyama, N. FOXO forkhead transcription factors induce G(2)-M checkpoint in response to oxidative stress. *J. Biol. Chem.* **2002**, *277* (30), 26729–26732.
(37) Dimmeler, S.; Fleming, I.; Fisslthaler, B.; Hermann, C.; Busse, R.; Zeiher, A. M. Activation of nitric oxide synthase in endothelial cells by Akt-dependent phosphorylation. *Nature* **1999**, *399* (6736), 601–605.
(38) Gao, F.; Gao, E.; Yue, T. L.; Ohlstein, E. H.; Lopez, B. L.; Christopher, T. A.; Ma, X. L. Nitric oxide mediates the antiapoptotic effect of insulin in myocardial ischemia-reperfusion: the roles of PI3-kinase, Akt, and endothelial nitric oxide synthase phosphorylation. *Circulation* **2002**, *105* (12), 1497–1502.
(39) Jones, S. P.; Greer, J. J.; Kakkar, A. K.; Ware, P. D.; Turnage, R. H.; Hicks, M.; van Haperen, R.; de Crom, R.; Kawashima, S.; Yokoyama, M.; Lefer, D. J. Endothelial nitric oxide synthase overexpression attenuates myocardial reperfusion injury. *Am. J. Physiol. Heart Circ. Physiol.* **2004**, *286* (1), H267–H282.
(40) Jones, S. P.; Greer, J. J.; van Haperen, R.; Duncker, D. J.; de Crom, R.; Lefer, D. J. Endothelial nitric oxide synthase overexpression attenuates congestive heart failure in mice. *Proc. Natl. Acad. Sci. U.S.A.* **2003**, *100* (8), 4891–4896.
(41) Scherrer-Crosbie, M.; Ullrich, R.; Bloch, K. D.; Nakajima, H.; Nasseri, B.; Aretz, H. T.; Lindsey, M. L.; Vancon, A. C.; Huang, P. L.; Lee, R. T.; Zapol, W. M.; Picard, M. H. Endothelial nitric oxide synthase limits left ventricular remodeling after myocardial infarction in mice. *Circulation* **2001**, *104* (11), 1286–1291.
(42) Potente, M.; Urbich, C.; Sasaki, K.; Hofmann, W. K.; Heeschen, C.; Aicher, A.; Kollipara, R.; DePinho, R. A.; Zeiher, A. M.; Dimmeler, S. Involvement of Foxo transcription factors in angiogenesis and postnatal neovascularization. *J. Clin. Invest.* **2005**, *115* (9), 2382–2392.

Received for review July 6, 2008. Revised manuscript received August 13, 2008. Accepted August 13, 2008. This study was supported by National Institutes of Health Grants HL 56803, HL 69910, and HL 85804.

JF802050H